Metastability of Nematic Gels Made of Aqueous Chitin Nanocrystal Dispersions

ARTICLE *in* BIOMACROMOLECULES · NOVEMBER 2009

Impact Factor: 5.75 · DOI: 10.1021/bm901046c · Source: PubMed

3 AUTHORS:

Maria V. Tzoumaki
Aristotle University of Thessaloniki
7 PUBLICATIONS **212** CITATIONS
SEE PROFILE

Thomas Moschakis
Aristotle University of Thessaloniki
28 PUBLICATIONS **548** CITATIONS
SEE PROFILE

Costas G. Biliaderis
Aristotle University of Thessaloniki
211 PUBLICATIONS **9,022** CITATIONS
SEE PROFILE

Metastability of Nematic Gels Made of Aqueous Chitin Nanocrystal Dispersions

Maria V. Tzoumaki, Thomas Moschakis, and Costas G. Biliaderis*

Department of Food Science and Technology, Laboratory of Food Chemistry and Biochemistry School of Agriculture, Aristotle University, GR-541 24, Thessaloniki, Greece

Received September 14, 2009; Revised Manuscript Received October 27, 2009

Chitin nanocrystal aqueous dispersions were prepared by acid hydrolysis of crude chitin from crab shells. The resulting dispersions were studied with small deformation oscillatory experiments and polarized optical microscopy under different conditions of nanocrystal concentration, ionic strength, pH, and temperature. The chitin nanocrystal dispersions exhibited a nematic gel-like behavior with increasing solids concentration. The appearance of nematic-like structures could be explained by the Onsager theory for parallel alignment of anisotropic particles on entropic terms, while the sol−gel transition could be attributed to associative interactions between the chitin nanocrystals. With increasing ionic strength and pH, such associative interactions were enhanced, because the repulsive forces due to the electrostatic charges were reduced and, thus, stronger gels were formed. Heating of the nanocrystal dispersions led to further increases in the storage modulus (G'), which were irreversible upon cooling; the rate of G' increase (dG'/dt) was dependent on temperature.

Introduction

Chitin, a structural polymer in shellfish, insects, and microorganisms, is the second most abundant polysaccharide found in nature and is composed of β-(1,4)-linked units of *N*-acetyl-D-glucosamine. Many authors have reported that acid hydrolyzed chitin preparations spontaneously disperse into rod-like crystalline particles that develop into rigid structures.[1–3] The stability of dilute colloidal dispersions of chitin nanocrystals has been attributed to the presence of positive charges at their surface, and this was suggested, arising from protonation of amino groups.[2] It has also been reported that such colloidal dispersions of acid-degraded chitin can undergo an isotropic−anisotropic nematic transition when their concentration is increased.[1–3] The phase separation in dispersions of these highly anisometric colloidal particles into an isotropic and a nematic phase has been addressed theoretically by Onsager.[4] He demonstrated that the stability of the nematic phase can be explained on purely entropic terms by considering the competition between orientational entropy (favoring the isotropic state) and excluded volume entropy (which favors the nematic state), which becomes more important at higher particle concentrations. It has also been found that above a certain concentration an aqueous dispersion of crystalline fragments from acid hydrolyzed chitin self-assemble to a cholesteric liquid crystalline phase,[2] which is another form of nematic organization. Moreover, Li et al.[5] studied the rheological properties of aqueous chitin nanocrystal dispersions and they observed a classical shear thinning behavior for isotropic dispersions and a three-regime curve for the anisotropic dispersions.

Dispersions of colloidal particles in aqueous media are widely investigated because of their use in many industrial applications (foods, pharmaceuticals, cosmetics, paints, etc.). Particularly in food systems, recent studies have emphasized the importance of the rheological and microstructural properties of colloidal particles on the bulk and surface properties of foods.[6,7] In addition, many particles of nanosized dimensions, like starch nanocrystals and chitin whiskers, have been used for the reinforcement of amorphous biopolymer matrices.[8,9]

Many anisotropic particles like cellulose nanocrystals,[10] boehmite rods,[11] and PBDT [poly(2,2′-disulfonyl-4,4′-benzidine terephthalamide)][12] display the isotropic−nematic transition under certain conditions (concentration, ionic strength, etc.), as mentioned in the case of the chitin nanocrystals. Several studies have been carried out on systems of anisotropic particles that present nematic gel-like behavior, like chitin nanocrystals,[3] boehmite rods,[13] gibbsite platelets,[14] and vanadium pentoxide ribbons.[15] Fewer studies have dealt with the dynamic rheological properties of such nematic gels, like clay particle gels with different shapes and sizes, hectorite, boehmite, and gibbsite,[16] nontronite,[17] and laponite colloidal disks.[18]

The mechanism of gel formation in these rod-like systems has been a matter of considerable debate, but it appears to be intimately related to the isotropic−nematic transition, as the microstructures of these concentrated gels closely resemble nematic network structures. Many authors have argued that attractive interactions that contribute to the network formation could be van der Waals forces.[15,19,20] Electrostatic interactions may also play a role in gel generation, although there are two conflicting views about them. First, some authors claim that attractions of electrostatic origin exist in colloidal particle systems due to repositioning of the counterions in the double layer,[21–23] while others claim that gelation of a colloidal dispersion could happen due to repulsive interactions; as the particles approach with an increase of concentration, their double layers overlap so that they are being "trapped" by neighboring particle repulsion, and the result is a yielding 3-D network structure.[13,24,25] The major variables that affect the rheological properties of such dispersions are particle concentration and factors which mediate the strength of interparticle interactions; that is, the nature of particles themselves (size, shape, and the distribution of these, aspect ratio and surface charge, among other characteristics), ionic strength, pH, and added soluble polymers.[16]

* Corresponding author. Tel. and Fax: +30-2310-991797. E-mail: biliader@agro.auth.gr.

10.1021/bm901046c
Published on Web 11/30/2009

To the best of our knowledge there are no available data regarding the viscoelastic properties of chitin nanocrystal nematic gels and additionally there is little work done on the thermo-irreversibility of gels consisting of rod-like particles, such as chitin nanocrystals. Therefore, the aim of the present study was to investigate the dynamic rheological behavior of chitin nanocrystal aqueous dispersions under different conditions of concentration, ionic strength, pH, and temperature. Also, complementary polarized optical micrographs have been taken in an attempt to relate the rheological and stability behavior to microstructural changes. Finally, the possible mechanisms behind the chitin nanocrystal nematic gel formation are being discussed. The current work illustrates that the gel-like character of aqueous dispersions of chitin nanocrystals is enhanced with increasing particle concentration, ionic strength, and pH. Furthermore, raising the temperature causes irreversible gel strengthening.

Experimental Section

Materials. Chitin from crab shells was obtained from Sigma Chemicals (St. Louis, MO). Hydrochloric acid (concentrated 37% v/v), sodium acetate, glacial acetic acid, potassium hydroxide, sodium chlorite, and sodium chloride were all of reagent grade and purchased from Sigma Chemicals (St Louis, MO). Double distilled water was used in all the experiments.

Chitin Nanocrystals Preparation. Aqueous stock dispersions of chitin nanocrystals were prepared from the original raw material of the crude chitin from crab shells based on the method described by Nair and Dufresne.[26] Approximately 30 g of chitin were suspended in 700 mL of 5% w/w KOH solution and boiled for 6 h under stirring to remove contaminating proteins. This dispersion was kept at room temperature overnight under continuous stirring and then filtered and washed several times with distilled water. The material remaining after the above procedure, was bleached in 700 mL of a $NaOCl_2$ solution (17 g of $NaOCl_2$ in 1 L of 0.3 M sodium acetate buffer, pH 4.0), at 80 °C for 6 h. The bleaching solution was changed every 2 h, followed by rinsing the sample with distilled water. Subsequently, the resulting material was kept in approximately 700 mL of 5% w/w KOH solution for 48 h to further remove residual proteins. The resulting dispersion was centrifuged at 3400 rpm for 15 min. The chitin nanocrystal dispersion was subsequently prepared by hydrolyzing the purified chitin sample with 3 N HCl at boil for 90 min under stirring. The ratio of 3 N HCl to chitin solids was 30 $cm^3\ g^{-1}$. After acid hydrolysis, the dispersion was diluted with distilled water and followed by centrifugation (3400 rpm for 15 min). This process was repeated three times. Afterward, the dispersion was transferred to a dialysis bag and dialyzed under running tap water for 2 h and then overnight under distilled water, and appropriate volumes of 1 N HCl solution were used to adjust the final pH of the dispersion to 3.0. To break the possible chitin nanocrystal aggregates, the dispersion was finally subjected to ultrasonic treatment (45 min for a 700 mL dispersion with 5 min intervals to avoid overheating of the sample; Ultrasons-H, P Selecta, Spain). The dispersions were subsequently stored at 4 °C after adding sodium azide (0.02% w/w) to avoid bacterial growth.

Sample Preparation. The solid chitin content of the stock dispersion was determined gravimetrically by drying the samples at 50 °C until a constant weight was obtained; the total solids content of the stock dispersion was approximately 3.6% w/w. Appropriate dilutions were made by using a solution of HCl, pH 3.0, to study the effect of concentration on the dispersion's properties. More concentrated samples were prepared by leaving the 3.6% w/w dispersion, at ambient temperature, for water evaporation.

Additionally, the effects of small electrolytes addition were investigated, using samples with different salt concentrations by mixing the stock chitin nanocrystal dispersion with appropriate quantities of the NaCl solutions; the final solids content was adjusted to 1.8% w/w. Also, the effect of pH was studied in dispersions prepared by mixing the stock chitin nanocrystal dispersion with acetate buffer solutions of different pH values; the final chitin nanocrystal concentration of the dispersions was maintained at 1.8% w/w and the final acetate buffer concentration was 50 mM for all samples.

The stock chitin nanocrystal dispersion was previously treated with ultrasound by placing 15 mL portions for 1 min in an ultrasound bath (Ultrasons-H, P Selecta, Spain) to disrupt any weakly formed aggregates before any treatments were applied. Sonication was also applied 15 min prior to any measurements.

Rheological Measurements. Rheological measurements of the samples were performed by a rotational Physica MCR 300 rheometer (Physica Messtechnic GmbH, Stuttgart, Germany) using a parallel sand-blasted plate geometry (to reduce the extent of wall slippage phenomena; 50 mm diameter and 1 mm gap); the temperature was regulated by a Paar Physica circulating bath and a controlled peltier system (TEZ 150P/MCR) with an accuracy of ±0.1 °C. To minimize dehydration, the samples were covered with a thin layer of silicone oil, and a solvent trap around the measuring geometry was also employed.

The linear viscoelastic region (LVR) was assessed at 1 Hz by amplitude sweep experiments; for all the chitin nanocrystal dispersions a constant deformation of $\gamma = 0.001$ was used, which was within the linear viscoelastic region for all the samples. Small deformation oscillatory measurements of the viscoelastic properties, G' (storage modulus), G'' (loss modulus), and tan δ (G''/G') were performed over the frequency range 0.01−10 Hz at 20 °C.

The thermoreversibility of the stock chitin nanocrystal structures was also studied. To explore the behavior of the chitin nanocrystal dispersion upon heating, a 3.6% w/w dispersion of chitin nanocrystals was heated from 20 to 86 °C at a scan rate of 3 °C/min; the samples were held at that temperature for 20 min and then cooled back to 20 °C at the same scan rate; this procedure was repeated twice. The experiments mentioned above were carried out at a constant frequency of 1 Hz.

Small deformation oscillatory experiments were performed at different temperatures, namely, 20, 32, 47, 62, and 86 °C ($\gamma = 0.001$, and 1 Hz), and the dynamic viscoelastic properties (G', G'') were studied as a function of time. An additional test was carried out at three different concentrations of chitin nanocrystals, namely, 2.4, 3.6, 4.6% w/w, at 62 °C. The samples have previously reached their respective target temperature with a scan rate of 3 °C/min.

Amplitude sweeps were also performed at frequency of 1 Hz and at 20 °C, in the range of 0.01−10 Pa of applied shear stress. Deviation from the linear viscoelastic region occurs when the sample starts to permanently deform, implying the destruction of the network structure. The apparent yield stress was calculated as the stress amplitude at which G' starts decreasing by 10% from the LVR, where the G' remains constant.

The yield stress, τ_y, was also quantified from the $\tau(\dot{\gamma})$ behavior of the dispersion, as determined by the Casson model treatment of the experimental data obtained from the flow curves performed at stresses ranging between 0.01 and 100 Pa.

$$\tau^{0.5} = \tau_y^{0.5} + K\dot{\gamma}^{0.5}$$

where τ is the shear stress (Pa), τ_y is the yield stress (Pa), K is the consistency index ($Pa^{0.5} \cdot s^{0.5}$), and $\dot{\gamma}$ is the shear rate.

Microscopy. Transmission electron microscopy imaging was performed on a JEOL JEM-2000FX transmission microscope operated at an acceleration voltage of 80 kV. One drop of the chitin nanocrystals suspension (0.02 w/w %) was deposited on a carbon-coated copper grid and allowed to air dry.

Optical micrographs of the chitin nanocrystal dispersions were captured by an Olympus BX 51 polarizing optical microscope fitted with a digital camera (Olympus, DP 50). The specimens were prepared by placing a thin layer of sample between a microscope slide and a coverslip.

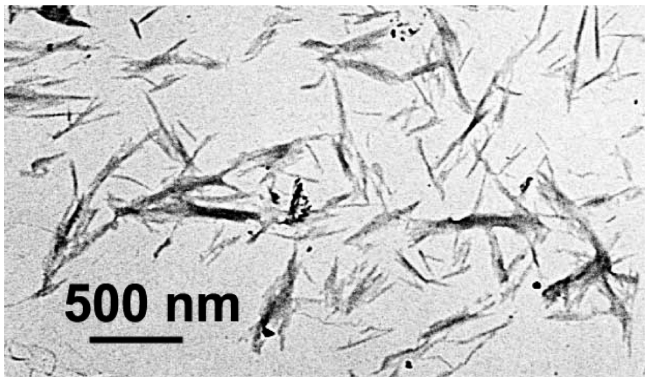

Figure 1. TEM micrograph of chitin nanocrystals formed after chitin hydrolysis.

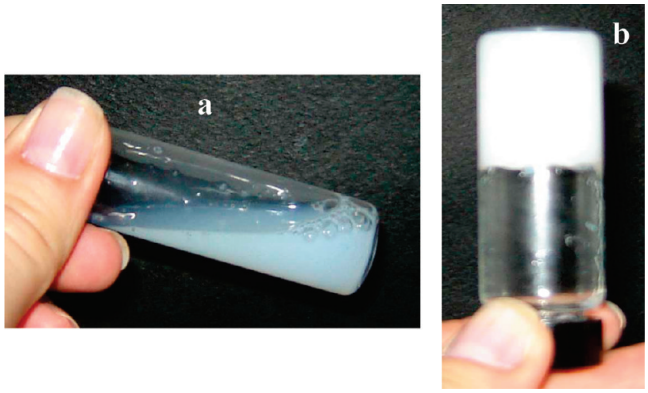

Figure 2. Chitin nanocrystal aqueous dispersions: (a) 1.8% w/w, liquid-like behavior; (b) 5% w/w, gel-like behavior.

Results and Discussion

The chitin nanocrystal dispersion contains chitin fragments which consist of slender rods with sharp points that have a broad distribution in particle size, as observed by transmission electron microscopy (Figure 1); average length and diameter were around 240 and 18 nm, respectively. Therefore, the average aspect ratio of nanocrystals, which were prepared for this study (L/d, L being the length and d the diameter) was around 13.5. Similar values for the chitin nanocrystals dimensions have been reported by Nair and Dufresne.[26]

Effect of Chitin Nanocrystal Concentration. The strength of the network structures was initially tested visually by tilting the sample tubes. It was observed that a 4.6% w/w aqueous dispersion of chitin nanocrystals did not flow when turning the test tube upside down, indicating a strong gel-like behavior, while the 1.8% w/w dispersion exhibited a viscous character (Figure 2). For an ideal gel that behaves elastically, the G' value is expected to be independent of frequency and $G' \gg G''$. As it can be seen from Figure 3a, for the 5% w/w dispersion, the G' was always higher than G'' in the frequency range explored, showing a weak power frequency dependence. However, at a lower concentration of 2.4% w/w, a viscous response was predominant with $G' < G''$ (Figure 3a). The gel state can be also characterized by the ratio of viscous to elastic character, that is, the loss tangent value ($\tan \delta = G''/G'$). When this value is <1, the system is characterized as an elastic gel. Increasing the chitin nanocrystal concentration led to an increase of the G' and the $\tan \delta$ decreased, as shown in Figure 3b. This indicates that the chitin nanocrystal dispersions shift from a viscous fluid to an elastic gel as the particle concentration increases.

The shear stress amplitude sweep tests for chitin nanocrystal dispersions of different solids concentrations are shown in Figure 4. It is observed that the higher the concentration the more extended the linear viscoelastic region, where the G' value remains relatively constant over a larger range of shear stress applied. The latter is also confirmed by the estimated yield stress values derived from the application of the Casson model (Table 1). Although the existence of yield stress has been questioned by many authors, it is a good indication of gel network strength.

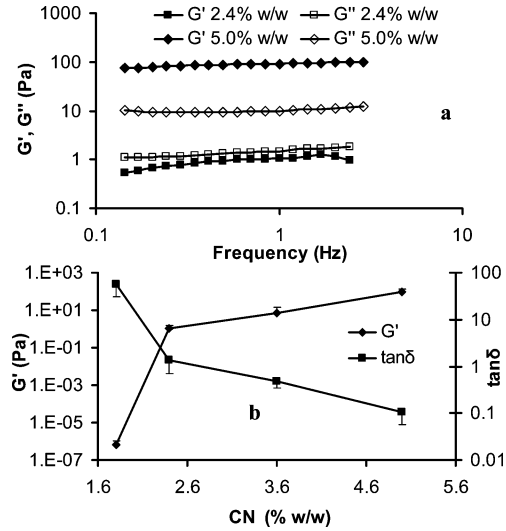

Figure 3. (a) Mechanical spectra of chitin nanocrystal aqueous dispersions (20 °C, $\gamma = 0.001$); (b) concentration dependence of elastic modulus (G') and tangent value ($\tan \delta$) of chitin nanocrystal dispersions (20 °C, frequency 1 Hz; CN, chitin nanocrystals; half bars represent ± S.D.).

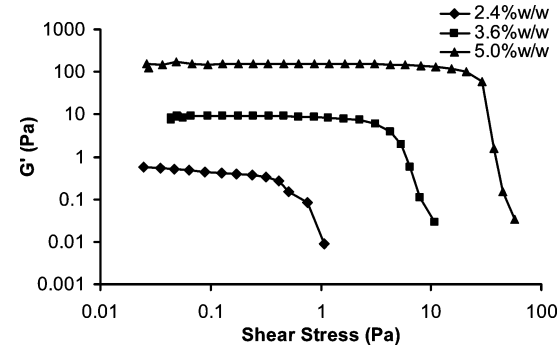

Figure 4. Shear stress amplitude sweeps (frequency 1 Hz, 20 °C) of dispersions containing different concentrations of chitin nanocrystals (2.4, 3.6, 5.0% w/w).

Micrographs obtained by polarized optical microscopy are presented for three different concentrations of aqueous chitin nanocrystal dispersions in Figure 5. The 2.4% w/w dispersion showed no or negligible birefringence, while the 3.6 and 4.6% w/w chitin nanocrystal dispersions exhibited birefringence (orientational ordering); the latter system also presented nematic thread-like structures. However, no clear cholesteric structures were observed, probably due to network formation which prevented the development of ordered particle aggregates as reported by Belamie et al.[3]

Several authors have noted that chitin nanocrystal dispersions have a nematic-type order beyond a critical volume fraction.[2,27,28] Even though it would be expected that positively charged nanocrystals form a stable colloidal dispersion, because of repulsive electrostatic forces, the system of chitin nanocrystals rapidly reaches thermodynamic equilibrium and exhibits a coexistence domain throughout the two phases, isotropic and nematic, which are separated by a sharp interface. The spon-

Table 1. Yield Stresses Calculated with Two Different Methods: Fitting of Casson Model and Amplitude Sweep

	yield stress in (Pa)			yield stress in (Pa)			yield stress in (Pa)	
effect of concentration (% w/w)	Casson model	amplitude sweep	effect of ionic strength (mM NaCl)	Casson model	amplitude sweep	effect of pH	Casson model	amplitude sweep
1.8	0.33		0	0.33		3.0	0.33	
2.4	0.34	0.41	5	0.37		4.0	2.72	5.91
3.6	1.62	4.26	15	1.94	4.25	4.6	3.12	8.03
5.0	2.12	28.8	34	2.33	4.27	5.3	2.91	11.10
			74	2.06	4.24	6.0	3.33	15.20
			100	3.66	8.09			

taneous phase separation of such dispersions of rod-like particles to give isotropic and nematic liquid crystalline phases was first studied by Zocher[29] and then Langmuir,[30] but Onsager[4] adequately rationalized the topic. The isotropic−nematic transition is purely entropic in nature. Although the orientational entropy of the system decreases due to alignment of the rods in the nematic phase, this loss is compensated by the increase in the positional or translational entropy of the system. In other words, the free volume available to individual rods increases as the rods align themselves, thus, resulting in an overall higher entropy of the system.[31]

Apart from the isotropic−liquid nematic phase transition in systems of anisotropic rod-like particles another phase may exist; that is, the nematic gel, which is usually formed with a further increase in particle concentration.[32] The literature abounds in systems of anisotropic moieties that display both gel and liquid-crystalline properties, like for boehmite rod dispersions and clay platelets.[11,13,20,33–36] However, the physical origin of the gelation process is not well understood, because it may involve different mechanisms depending on the type of interactions operating in such systems, for example, repulsive gels or attractive gels.[13,20,36]

Regarding chitin nanocrystal dispersions, it has been reported that a physical gel could be formed in concentrations above 10−13% by some authors,[2,5] while Belamie et al.[3] have reported gel formation of chitin nanocrystals over a wider range of concentrations (approximately 1.5−6% w/w), but at relatively high HCl concentration (above 10^{-2} M HCl), which hinders the sedimentation of the nematic droplets and inhibits the bulk phase separation. At lower HCl concentrations, a typical isotropic−nematic transition was observed.[3]

As previously shown by the viscoelastic responses and the optical microscopic observations, in the present system, a sol−nematic gel transition is evident in chitin nanocrystal dispersions with increasing solids concentration. One reason for network formation could be the van der Waals attraction forces between the parallel aligned rods, but further investigation is needed. That is, as the volume fraction of nanocrystals increases, the aggregated rods come to shorter distances, thus, increasing the magnitude of van der Waals interactions, leading to a stronger gel network with a nematic-like structure. Indeed, many systems of anisotropic particles, as reported in the literature,[15,18,20,37] are characterized by strong van der Waals attractions between the rod-like nanocrystals, which lead to the formation of aggregates and bundles of the dispersed particles. Even when the attraction between two nearly touching-crossed rods is weak, its effect can become sizable in the case of rods adapting a parallel configuration.[19] Apart from the van der Waals forces that could explain to a certain extent the nematic gel formation, there has been a considerable debate for the interactions present in these gels as summarized by the following two conflicting models. On the one hand, it has been suggested that the formation of a three-dimensional network is governed by electrostatic attractions between the charged particles.[23,32,38] That is, as two highly charged particles approach with the increase of concentration, the counterion clouds around these particles may reposition in response to the altered electrical field. When such fluctuations in the counterion clouds of the two surfaces of particles are accounted for, an attractive rather than a repulsive interaction is reported.[23,32,38] On the other hand, gelation of a colloidal dispersion has been argued to be attributed to repulsive interactions. If the colloidal particles are surrounded by extensive double layer, double layer overlap may strongly reduce particle diffusion, leading to the formation of a stiff repulsive gel, like in the case of rod-like or plate-like particles.[13,14,24]

Effect of Ionic Strength. The influence of ionic strength in chitin nanocrystals properties was determined by small deformation measurements. In this case, distilled water in the dispersions was replaced by different NaCl solutions, to obtain final NaCl concentrations between 5 and 100 mM, at a nanocrystals concentration of 1.8% w/w.

In Figure 6a, G' and tan δ were plotted against NaCl concentrations (at 1 Hz and 20 °C). As the sodium chloride concentration increases, the dispersion shifts from viscous to elastic response. Above 5 mM NaCl, the 1.8% w/w chitin nanocrystal dispersions have a dominant elastic character (tan $\delta < 1$), while the salt-free dispersion is predominantly viscous. This indicates that associative forces are dominating in the system leading to network formation by the chitin nanocrystals. The associative interactions could be attributed to the electrostatic screening of the chitin nanocrystal double layer by the salt addition, which leads to minimization of the

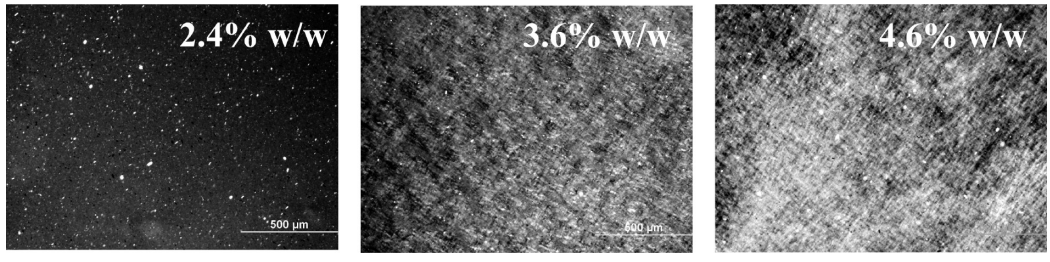

Figure 5. Polarized optical micrographs of aqueous dispersions containing different concentrations of chitin nanocrystals (2.4, 3.6, 4.6% w/w; scale bar 500 μm).

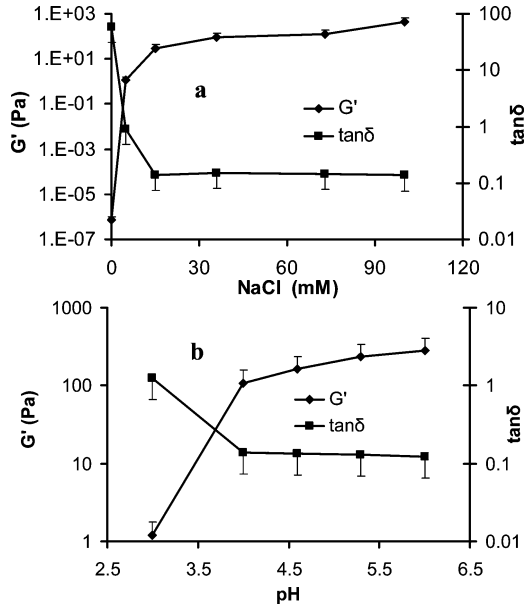

Figure 6. (a) Variation of G' and tan δ of chitin nanocrystal aqueous dispersions (1.8% w/w, 20 °C, frequency 1 Hz) as a function of NaCl concentration; (b) variation of G' and tan δ of chitin nanocrystal dispersions (1.8% w/w, 20 °C, frequency 1 Hz) as a function of pH (half bars represent ± S.D.).

repulsive forces due to the electrostatic charge of the nanocrystals. These attractive forces that contribute to network formation could be either of electrostatic origin or even van der Waals interactions, as discussed in the previous section. Additionally, the yield stress values (Table 1) did increase with increasing the ionic strength above 15 mM NaCl. The highest value was obtained for the chitin nanocrystal dispersions with 100 mM NaCl, indicating again the greater impact of salt addition on the dispersions' rheological responses.

As shown in the micrographs of Figure 7a, the salt-free 1.8% w/w chitin nanocrystal dispersion did not exhibit any birefringence, while the dispersions containing 15 and 100 mM NaCl resembled a birefringent microstructure with increasing salt concentration. It is also worth noting that the 100 mM NaCl chitin nanocrystal dispersion demonstrates an inhomogeneous structure with some dark nonbirefringent voids, showing a different structural organization from the higher chitin nanocrystal concentration sample (4.6% w/w, without salt) of Figure 5, which exhibits a more intense birefringence. These voids present in the sample indicate flocculation, but still, this sample behaves as a gel according to the rheological responses observed.

Similar results have been obtained in a previous study involving addition of salt (above 10^{-2} M) in chitin nanocrystal dispersions,[3] where the system did not phase separate in isotropic and anisotropic phases; these samples did not flow spontaneously when tilting the test tubes. Observations with polarizing microscopy revealed the presence of very small birefringent droplets that grew in size and eventually lead to a continuous highly defected nematic phase. Moreover, Lowys et al.[39] have found that, for cellulosic microfibril dispersions, the higher the sodium chloride concentration, the stronger the gel-like behavior.

Different behavior was described for colloidal gels of anisotropic particles, where their network formation without added salts was attributed to repulsive interactions.[13,14,34] In relatively low salt concentrations, the dominant particle interactions are repulsive, and the increase of the ionic strength leads to a reduction of the double layer interactions, causing a breakup of the gels and the formation of some flocs. At intermediate salt concentration, however, there is a balance between repulsive and attractive interactions. As soon as the number of flocculated rods is high enough to form a space-filling structure, a new gel could be formed, consisting of a network of aggregated particles in a dispersion of stable particles. Further increases in the ionic strength can render the behavior dominated by particle attractions. Reorientation of anisotropic particles in clusters to form parallel aggregates then induces a denser network structure, causing syneresis and a concomitant decrease of the yield stress.[13,14,34]

Effect of pH. Similar responses to those obtained with varying the ionic strength were noted for the effect of pH. As it can be seen in Figure 6b, with increasing pH, the chitin nanocrystal dispersions exhibited a stronger gel-like behavior; that is, the G' value increases and the tan δ decreases. Additionally, the yield stress value increases with the pH, as shown in Table 1. The isoelectric point of chitin nanocrystal dispersions is reported around 6.3[2]; therefore, as the pH reaches lower values, for example, pH 3.0, the chitin nanocrystal amino groups should be totally protonated. The electrostatic repulsive forces at this pH level and a low chitin nanocrystal concentration (1.8% w/w) would inhibit the network formation. In contrast, when the dispersion approaches the pH value of 6.3, the repulsive electrostatic forces are minimized and the nanocrystals could then easily aggregate and form a gel.

The cross-polarized microscopic images of the chitin nanocrystal dispersions at different pH levels confirmed a network generation as the pH gets closer to the isoelectric point of chitin dispersions (6.3); that is, the sample with pH 3.0 shows no birefringence, while at a pH 6.3 the dispersion exhibits a birefringent nematic-like structure (Figure 7b).

Effect of Temperature. The influence of temperature on the behavior of chitin nanocrystal dispersions was studied by repeating a heating and cooling protocol on a 3.6% w/w dispersion from 20 to 86 °C, as shown in Figure 8. Heating the chitin nanocrystal dispersions resulted in an increase in the elastic modulus, which continued to rise as the temperature was kept at 86 °C. Upon cooling, the value of G' remained relatively constant at the level obtained upon heating; that is, the change caused by heating is irreversible. Throughout the second heating and cooling cycle, the sample exhibited similar behavior as above, although the stepwise increase in the G' values was lower. The change in the structure of chitin nanocrystal dispersion caused by heating was also reflected in the images obtained from the polarizing optical microscope, where the unheated sample of the 2.8% w/w dispersion shows little birefringence, while its heated counterpart exhibited a birefringent nematic-like structure (Figure 9).

The influence of temperature on the chitin nanocrystals structure was further studied by examining isothermally the 3.6% w/w samples at different temperatures, from 20 to 86 °C. Figure 10 shows the time-dependence of the storage modulus, stored at different temperatures. As it can be seen, there is a large increase in the elastic modulus (G') with increasing temperature. Moreover, the rate of G' increase (dG'/dt) raises with temperature (Figure 10). The data collected after the target temperature was reached could be described by an exponential growth rate response (inset Figure 10). It is noticeable that even at 20 °C the elastic modulus increased with time, indicating that the chitin nanocrystal dispersions following sonication are not stable and they probably reorganize to a stronger structure, as it was observed in the case of boehmite rods gels[13] and gibbsite platelets.[24]

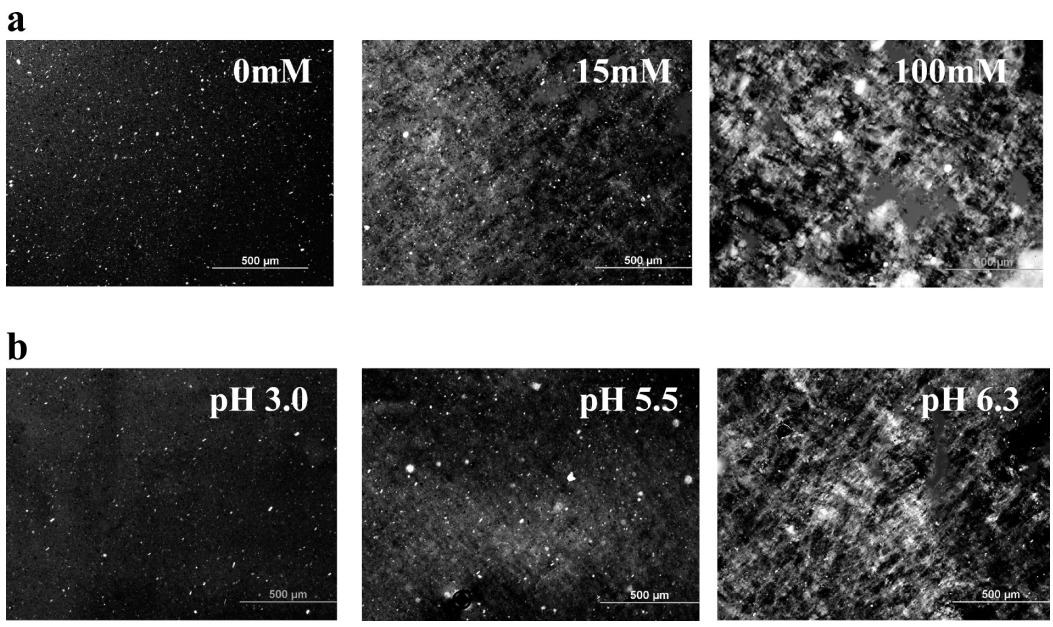

Figure 7. (a) Effect of ionic strength on the microstructure of a 1.8% w/w chitin nanocrystal aqueous dispersion; (b) effect of pH on the microstructure of a 1.8% w/w chitin nanocrystal aqueous dispersion (scale bar 500 μm).

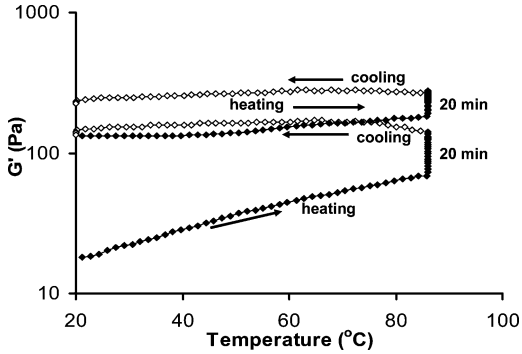

Figure 8. Effect of heating and cooling cycles on the elastic modulus (G') of a 3.6% w/w chitin nanocrystal aqueous dispersion; heating and cooling rate 3 °C/min, frequency 1 Hz.

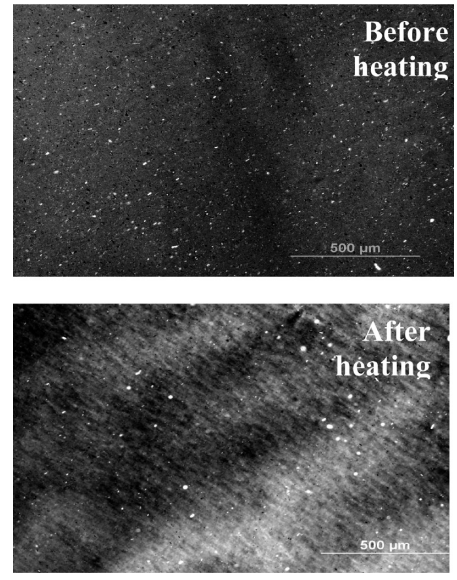

Figure 9. Effect of heating on the microstructure of a 2.8% w/w chitin nanocrystal aqueous dispersion at 86 °C for 2 h (scale bar 500 μm).

Additionally, the time-dependence of G' for dispersions of different chitin nanocrystal concentrations was examined at a constant temperature (e.g., 62 °C, Figure 11). It seems that the higher the solids content the greater the rate of the storage modulus evolution, implying stronger associative interactions (data collected from the part of the graphs after the target temperature was reached). Similar results were also observed for the time-dependence of the G' of dispersions with different NaCl concentrations, stored at constant temperature of 62 °C; that is, with higher salt concentration, a greater value of dG'/dt is observed, showing that as the interparticle distances decrease, due to screening of the double layer, the interparticle interactions become stronger (data not shown).

All the above observations indicate the increasing influence of associative interactions with the temperature. As already mentioned, the chitin nanocrystal dispersions are not stable with time even at 20 °C, and as the particles tend to realign to give a stronger structure, heating seems to accelerate this process since the kinetic energy of the particles is enhanced and thus they become more mobile to rearrange themselves; that is, the higher the temperature the greater the rate of structure formation, as shown in Figure 11. Additionally, with increasing temperature, the kinetic energy of the counterions is enhanced and, thus, the diffuse-double layer thickness is reduced. As a result, the interparticle distances are decreased, microflocculation can occur, and the associative forces between the nanocrystals are strengthened. There are few studies reporting the effect of heating on the behavior of anisotropic gels. Thermal contraction of crystalline arrays has been observed by Ise and Smalley,[40] who attributed such liquid crystalline compression to the temperature dependence of the Debye screening length, k^{-1}. As previously discussed, the attractive forces that may lead to gel formation from charged rod-like particles, like chitin nanocrystals, may be van der Waals forces,[19,37] which become more intense as the rods align themselves and as their distances are reduced, or forces of electrostatic nature due to rearrangement of the counterions on the surfaces of the charged particles.[21,23,32] We argue here that the attractive interactions, which are dominant in the present system of chitin nanocrystal aqueous dispersions, are most probably van der Waals forces, because the changes observed upon heating were irreversible. This is further supported by the average interparticle distance values,

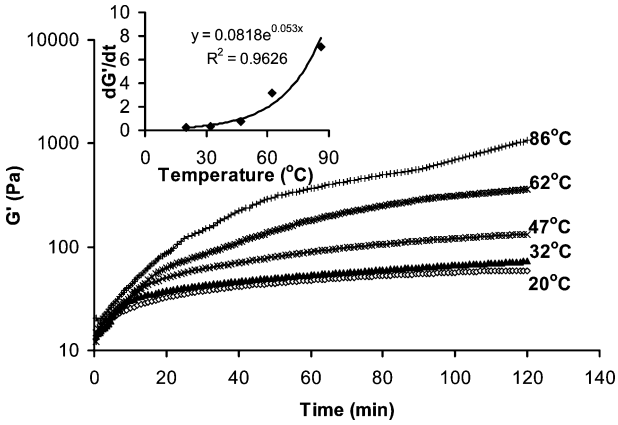

Figure 10. Kinetic responses of storage modulus for a chitin nanocrystal aqueous dispersion (3.6% w/w) maintained at different temperatures (frequency 1 Hz), and the exponential equation fitting the rate of G' increase (dG'/dt) with temperature (inset).

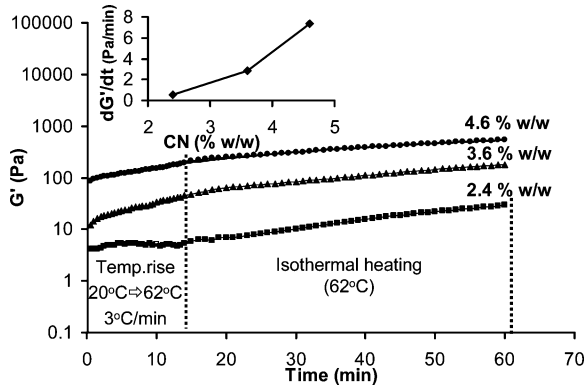

Figure 11. Time dependence of G' evolution for aqueous dispersions of chitin nanocrystals at different concentrations (62 °C, frequency 1 Hz); CN-chitin nanocrystals.

in the range of 60−120 nm, for chitin particle dispersions in the anisotropic phase (in planes perpendicular to the director), as recently reported by small-angle X-ray scattering measurements;[3] for such a distance scale, the van der Waals forces become predominant.

Conclusions

The chitin nanocrystal aqueous dispersions shifted toward a nematic gel-like behavior with increasing solid particle concentration. These nanocrystals, at a pH 3.0, being charged rod-like colloids, form parallel configurations as their volume fraction is increased for entropic reasons, as predicted by Onsager.[4] Alignment of the particles seems to foster attractive interactions, mainly of van der Waals type. With increasing ionic strength and pH, such attractive interactions were enhanced, because the repulsive forces of electrostatic origin were reduced and stronger gels were thus formed. By heating the nanocrystal dispersions, an increase in storage modulus was observed, which was irreversible upon cooling, and the rate of increase depended on temperature. These findings led to the conclusion that the attractive interactions are enhanced by increasing the temperature, possibly by suppression of the double layer and thereby decreasing the interparticle distances. Additionally, it has been found that the gel strength increases with time and the nanocrystal rods reorient to stronger network structures, thus pointing to the metastable nature of the chitin nanocrystal gels.

Acknowledgment. The authors thank Professor N. Frangis (Department of Physics, Aristotle University of Thessaloniki) for providing the transmission electron micrographs. M.V.T. also thanks the State Scholarship Foundation (IKY) for awarding her a graduate fellowship.

References and Notes

(1) Marchessault, R. H.; Morehead, F. F.; Walter, N. M. *Nature* **1959**, *184*, 632–633.
(2) Revol, J. F.; Marchessault, R. H. *Int. J. Biol. Macromol.* **1993**, *15*, 329–335.
(3) Belamie, E.; Davidson, P.; Giraud-Guille, M. M. *J. Phys. Chem. B* **2004**, *108*, 14991–15000.
(4) Onsager, L. *Ann. N. Y. Acad. Sci.* **1949**, *51*, 627–659.
(5) Li, J.; Revol, J. F.; Marchessault, R. H. *J. Colloid Interface Sci.* **1996**, *183*, 365–373.
(6) Moschakis, T.; Murray, B. S.; Dickinson, E. *Langmuir* **2006**, *22*, 4710–4719.
(7) Nayebzadeh, K.; Chen, J. S.; Dickinson, E.; Moschakis, T. *Langmuir* **2006**, *22*, 8873.
(8) Kristo, E.; Biliaderis, C. G. *Carbohydr. Polym.* **2007**, *68*, 146–158.
(9) Lu, Y. S.; Weng, L. H.; Zhang, L. N. *Biomacromolecules* **2004**, *5*, 1046–1051.
(10) Dong, X. M.; Kimura, T.; Revol, J. F.; Gray, D. G. *Langmuir* **1996**, *12*, 2076–2082.
(11) Buining, P. A.; Lekkerkerker, H. N. W. *J. Phys. Chem.* **1993**, *97*, 11510–11516.
(12) Shigekura, Y.; Furukawa, H.; Yang, W.; Chen, Y. M.; Kaneko, T.; Osada, Y.; Gong, J. P. *Macromolecules* **2007**, *40*, 2477–2485.
(13) Wierenga, A.; Philipse, A. P.; Lekkerkerker, H. N. W.; Boger, D. V. *Langmuir* **1998**, *14*, 55–65.
(14) Mourad, M. C. D.; Wijnhoven, J.; van't Zand, D. D.; van der Beek, D.; Lekkerkerker, H. N. W. *Philos. Trans. R. Soc., A* **2006**, *364*, 2807–2816.
(15) Pelletier, O.; Davidson, P.; Bourgaux, C.; Livage, J. *Europhys. Lett.* **1999**, *48*, 53–59.
(16) ten Brinke, A. J. W.; Bailey, L.; Lekkerkerker, H. N. W.; Maitland, G. C. *Soft Matter* **2007**, *3*, 1145–1162.
(17) Michot, L. J.; Baravian, C.; Bihannic, I.; Maddi, S.; Moyne, C.; Duval, J. F. L.; Levitz, P.; Davidson, P. *Langmuir* **2009**, *25*, 127–129.
(18) Cocard, S.; Tassin, J. F.; Nicolai, T. *J. Rheol.* **2000**, *44*, 585–594.
(19) van der Schoot, P. *J. Phys. Chem.* **1992**, *96*, 6083–6086.
(20) van Bruggen, M. P. B.; Lekkerkerker, H. N. W. *Langmuir* **2002**, *18*, 7141–7145.
(21) Ise, N. *Angew. Chem., Int. Ed.* **1986**, *25*, 323–334.
(22) Larsen, A. E.; Grier, D. G. *Nature* **1997**, *385*, 230–233.
(23) Sogami, I.; Ise, N. *J. Chem. Phys.* **1984**, *81*, 6320–6332.
(24) Mourad, M. C. D.; Byelov, D. V.; Petukhov, A. V.; Lekkerkerker, H. N. W. *J. Phys.: Condens. Matter* **2008**, *20*, 494201.
(25) Gabriel, J. C. P.; Sanchez, C.; Davidson, P. *J. Phys. Chem.* **1996**, *100*, 11139–11143.
(26) Nair, K. G.; Dufresne, A. *Biomacromolecules* **2003**, *4*, 657–665.
(27) Revol, J. F.; Bradford, H.; Giasson, J.; Marchessault, R. H.; Gray, D. G. *Int. J. Biol. Macromol.* **1992**, *14*, 170–172.
(28) Li, J.; Revol, J. F.; Naranjo, E.; Marchessault, R. H. *Int. J. Biol. Macromol.* **1996**, *18*, 177–187.
(29) Zocher, H. *Z. Anorg. Allg. Chem.* **1925**, *147*, 91.
(30) Langmuir, I. *J. Chem. Phys.* **1938**, *6*, 873–896.
(31) Beck-Candanedo, S.; Viet, D.; Gray, D. G. *Macromolecules* **2007**, *40*, 3429–3436.
(32) McBride, M. B.; Baveye, P. *Soil Sci. Soc. Am. J.* **2002**, *66*, 1207–1217.
(33) Davidson, P.; Batail, P.; Gabriel, J. C. P.; Livage, J.; Sanchez, C.; Bourgaux, C. *Prog. Polym. Sci.* **1997**, *22*, 913–936.
(34) van der Beek, D.; Lekkerkerker, H. N. W. *Europhys. Lett.* **2003**, *61*, 702–707.
(35) Philipse, A. P.; Nechifor, A. M.; Patmamanoharan, C. *Langmuir* **1994**, *10*, 4451–4458.
(36) Buining, P. A.; Philipse, A. P.; Lekkerkerker, H. N. W. *Langmuir* **1994**, *10*, 2106–2114.
(37) Surve, M.; Pryamitsyn, V.; Ganesan, V. *Macromolecules* **2007**, *40*, 344–354.
(38) Belloni, L. *J. Phys.: Condens. Matter* **2000**, *12*, R549–R587.
(39) Lowys, M. P.; Desbrieres, J.; Rinaudo, M. *Food Hydrocolloids* **2001**, *15*, 25–32.
(40) Ise, N.; Smalley, M. V. *Phys. Rev. B* **1994**, *50*, 16722–16725.

BM901046C